Ab initio study of the physical properties of binary Si_mC_n ($m+n \leq 5$) nanoclusters

2006 J. Phys.: Condens. Matter 18 7085

(http://iopscience.iop.org/0953-8984/18/31/004)

INSTITUTE OF PHYSICS PUBLISHING JOURNAL OF PHYSICS: CONDENSED MATTER

J. Phys.: Condens. Matter **18** (2006) 7085–7102 doi:10.1088/0953-8984/18/31/004

Ab initio study of the physical properties of binary Si_mC_n ($m + n \leqslant 5$) nanoclusters

P S Yadav, R K Yadav, S Agrawal and B K Agrawal

Physics Department, Allahabad University, Allahabad-211002, India

E-mail: balkagr@yahoo.co.in and balkagl@rediffmail.com

Received 28 February 2006, in final form 28 June 2006
Published 21 July 2006
Online at stacks.iop.org/JPhysCM/18/7085

Abstract

An *ab initio* study of the stability, structural, electronic, vibrational and optical properties of the most stable silicon–carbon binary nanoclusters Si_mC_n ($m+n \leqslant 5$) has been made. A B3LYP-DFT/6-311G(3df) method has been employed to optimize fully the geometries of the nanoclusters. The binding energies (BEs), highest occupied molecular orbital (HOMO)–lowest unoccupied molecular orbital (LUMO) gaps, bond lengths, ionization potentials (IPs), adiabatic electron affinities (EAs), vibrational frequencies, infrared intensities, relative infrared intensities and Raman scattering activities have been computed. In the more stable structures, the carbon atoms are in the majority whereas in the less stable structure the reverse is true. For the clusters containing all the carbon atoms except one silicon atom, the BE increases monotonically with the number of carbon atoms. The ground states of the clusters containing even numbers of the carbon atoms are, in general, lower than those containing odd numbers of carbon atoms. On the other hand, the lowest unoccupied states of the clusters containing even numbers of carbon atoms lie higher than those containing odd numbers of carbon atoms. All the predicted physical quantities are in good agreement with the experimental data wherever available. The growth of these most stable structures should be possible in the experiments.

1. Introduction

The study of the physical properties of nanoclusters has drawn great attention in recent years as their properties are different from those of the bulk material. Over the last several years, semiconductor clusters specially, the silicon and carbon clusters have been the subject of intensive studies [1–5]. The atomic cluster is an intermediate phase between the single atom and the bulk material. It is of great interest to understand how the atomic and electronic properties of the clusters change with their size. A comparative study of the dynamical properties of silicon, germanium and carbon clusters has been reported by Lu *et al* [6].

Silicon carbide is a wide-bandgap semiconductor and is an attractive material from the technological point of view [7] due to its high potential in electrical [8] and high temperature mechanical [9] devices.

The structures and the physical properties of the mixed silicon–carbon hetero-clusters have attracted much attention over the past several years. One of the main reasons for this study is that SiC, SiC_2, SiC_3, and SiC_4 clusters have been detected in interstellar space and in the atmosphere of carbon stars [10–14]. Their detection, therefore, is important for an understanding of the chemical processes in the interstellar environments, and their discovery has inspired several workers to produce them in the laboratory [15–18].

Even though carbon and silicon are contiguous in the same column (Group IV) of the periodic table, their chemical and bonding properties are quite different. While carbon exhibits huge flexibility by forming single and multiple bonds, this characteristic is not shared by silicon, which prefers multidirectional single bonds. The different behaviour in the bonding is reflected in the structures of small pure clusters. Small carbon clusters C_n ($n \leqslant 10$) form planar structures, linear for odd n and cyclic for even n [19–21]. In contrast, silicon Si_m clusters are known to prefer three-dimensional structures starting with m as small as $m = 5$ [22–25]. These striking differences are also evident in the bulk phase, since no graphite structure exists for Si. In the intermediate size silicon–carbon clusters, it is reasonable to expect to find a transition from carbon-like to silicon-like behaviour as we go from carbon-rich to silicon-rich clusters. This trend has been confirmed experimentally in previous works [26–29].

The SiC molecule has been predicted by various chemical models to be abundant in dense interstellar clouds [30] and stellar atmospheres [31, 32].

For example, Suzuki [30] reported that under steady-state conditions SiC is more abundant than SO, which is widely observed. The SiC_2 molecule also occurs widely in stellar atmospheres [33–35] and has recently been detected in the interstellar medium [11]. For many years, the SiC_2 molecule was considered to be linear like C_3, but Michalopoulos *et al* [36] proved that SiC_2 had a triangular structure.

It is very important to understand how the semiconductor binary clusters like Si_mC_n (where $m + n \leqslant 5$) can be created in the experiments under certain conditions. One might anticipate that there should be interesting properties existing for the binary Si_mC_n nanoclusters. The study of the semiconductor binary nanoclusters may provide insight into the bulk alloy structures. Although some theoretical and experimental studies of Si_mC_n binary nanoclusters have been reported in the literature, a detailed theoretical study of the variation of the physical properties with the size of the nanocluster is not available.

Earlier, the physical and vibrational properties of the semiconducting binary clusters were investigated by using semiempirical techniques, Hartee–Fock (HF) and local density approximation (LDA) methods. Li *et al* [37] have investigated the nanoclusters A_mB_n (A, B = Si, Ge) for $m + n \leqslant 10$ using the B3LYP-DFT method and have studied only some Si_mC_n clusters.

In the present paper, we make a comprehensive detailed study of the stability, structural, electronic, vibrational, optical and Raman active properties of the small semiconductor binary Si_mC_n ($m + n \leqslant 5$) nanoclusters by using the B3LYP-DFT method. Our results for the structures of the clusters are in agreement with the available experimental data and also with those of the earlier workers. We predict here a number of new cluster configurations; some of them are seen to be highly stable but are not reported in the literature.

2. Method

The atomic orbitals which are named the contracted functions are formed by making a linear combination of Gaussian functions. For a precise calculation, a large basis set is chosen by

increasing the number of basis functions per atom. 6-311G is a triple split valence basis set which uses three sizes of the contracted functions for each orbital type. The split valence basis set allows orbitals to change size but does not permit change in the shape of the orbitals. In order to remove this limitation, we employ a polarized basis set, 6-311G (3df) by adding orbitals with angular momentum beyond what is required for the ground state in the description of each atom. Here we add 3d functions to the carbon atoms and one f function to the silicon atom. Both the triple zeta basis set and the multiple polarization functions have been used to generate quite accurate structural parameters.

In the DFT, the exact exchange in the Hartree–Fock theory for a single determinant is replaced by a more general expression, the exchange–correlation functional, which can include terms accounting both for the exchange energy and the electron correlation.

In BLYP one includes the Becke exchange functional and the LYP correlation functional, whereas in B3LYP one includes Becke [38] three parameter hybrid functionals and the LYP correlation functional. The correlation function of Lee, Yang and Parr (LYP) [39, 40], which includes both local and nonlocal terms, has been employed. The functional of Becke which includes the Slater exchange along with the corrections involving the gradient of the density [38] is used.

The B3LYP-DFT/6-311G(3df) version in the Gaussian-03 code [41] has been used to optimize the geometries of the silicon–carbon binary nanoclusters. The Gaussian programme contains the hierarchy of procedures corresponding to different approximation methods.

3. Calculation and results

3.1. Stability of structures

We study all the various types of structures including the linear chain, ring, planar and three-dimensional ones. The atomic positions were relaxed to achieve the minimum energy. The system energy has been converged up to 10^{-3} meV. The atomic positions were optimized till the forces were as small as 10^{-3} eV $Å^{-1}$ on any atom.

We define the binding energy of a cluster as follows: the total energy of a cluster is subtracted from the total energy of all the isolated atoms in the cluster and this change in energy is divided by the number of atoms in the cluster. This quantity is called the binding energy (BE) per atom. For a more precise calculation, we have calculated the harmonic vibrational frequencies and the corresponding zero point energies have been subtracted from the earlier calculated BE values. Among all the complexes pertaining to a specific chemical formula Si_mC_n, the configuration possessing the maximum value of BE is named as the most stable structure.

In figures 1–7, we present 41 optimized structures. The C–C, Si–C and Si–Si bond lengths and bond energies calculated in isolation are 1.301, 1.713 and 2.159 Å, and 6.22, 4.36 and 3.08 eV, respectively. The experimental values [42] of the dissociation energies for the C–C, Si–C and Si–Si bonds are 6.23, 4.60 and 3.24 eV, respectively. The calculated values of the C–C, Si–C and Si–Si bond lengths are in excellent agreement with the measured values [13, 42] of 1.312, 1.731 and 2.246 Å, respectively. The same is true for the various bond energies.

One may expect the minimum energies for those complexes which contain the maximum number of C–C bonds followed by Si–C and Si–Si bonds.

The calculated BEs and HOMO–LUMO gaps are given for all the 41 optimized structures in table 1. On the other hand, the IPs and EAs for the most stable ones are included in table 1. The most stable structures have been depicted in bold letters.

For the most stable structures the calculated Si–Si, Si–C and C–C bond lengths are compared with the available experimental data and those of the others in table 2.

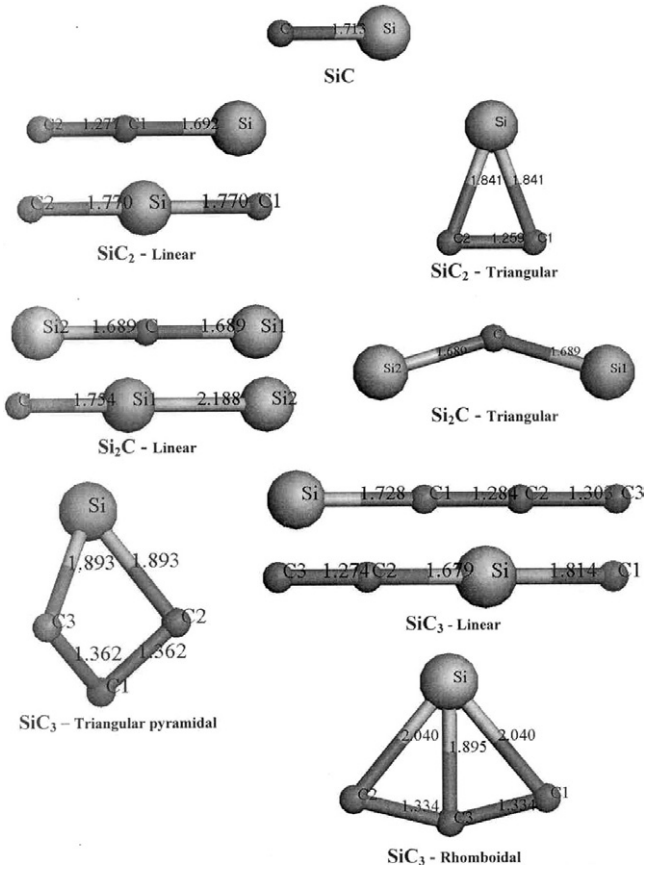

Figure 1. Optimized structures of SiC, SiC_2, Si_2C and SiC_3 nanoclusters.

We now discuss each cluster individually in the following:

SiC. The ground state of the SiC cluster is the triplet state and the singlet state lies above it at 1.17 eV. The calculated BE after considering the zero point energy of the linear SiC structure is 2.12 eV, which is close to the experimental upper limit of 2.30 eV [42]. The experimental value [42] of the dissociation energy is 4.60 eV for the cluster of two atoms, whereas here we have calculated the binding energy per atom. The calculated bond length of the linear SiC cluster (1.713 Å) is in good agreement with the experimental value (1.731 Å) [13].

Si_mC_n $(m + n = 3)$

The ground states of all the linear and triangular structures are singlets.

SiC_2. We have considered the linear configurations Si–C–C, C–Si–C and a triangular configuration. The linear structures have $C_{\infty v}$ (Si–C–C) and $D_{\infty h}$ (C–Si–C) symmetries whereas the triangular structure has C_{2v} symmetry. Among them, the linear (Si–C–C) and the triangular structures have equal binding energies (4.08 eV). We find that the BE of linear SiCC is greater than that of CSiC. For the linear (Si–C–C) structure, our calculated Si–C and C–C bond lengths are close to those reported by others [43, 44]. The present EA (1.50 eV) for the linear SiCC structure is quite close to the available experimental value of 1.37 eV [27].

For the triangular structure, the present Si–C and C–C bond lengths are in good agreement with the experimental values [11, 36] as shown in table 2. The other authors have also reported

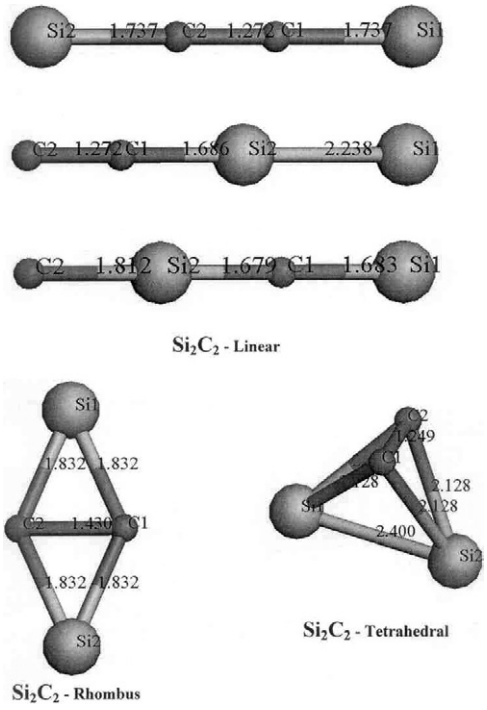

Figure 2. Optimized structures of Si_2C_2 nanoclusters.

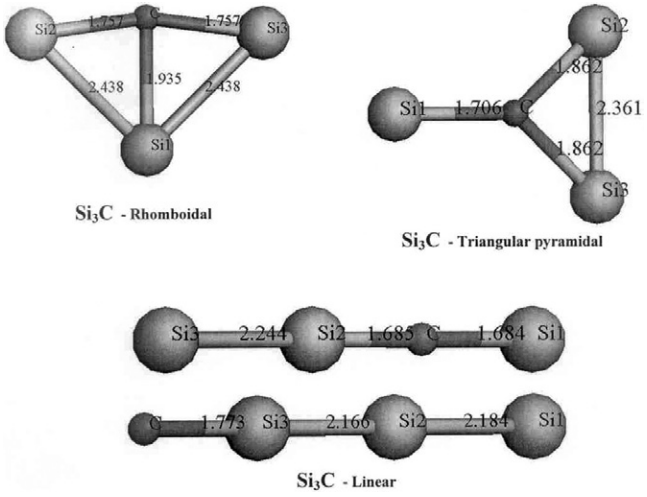

Figure 3. Optimized structures of Si_3C nanoclusters.

quite similar values [37, 43, 44]. The currently calculated bond angle CSiC of 40° for the triangular structure is in excellent agreement with the experimental value of 40.4° [11, 36].

Si_2C. Here the studied configurations are similar to SiC_2. Again, one (Si–C–Si) linear structure and the triangular structures have quite similar binding energies. The BE of the linear SiCSi is greater than that of the linear SiSiC. For the triangular structure, the present Si–C and

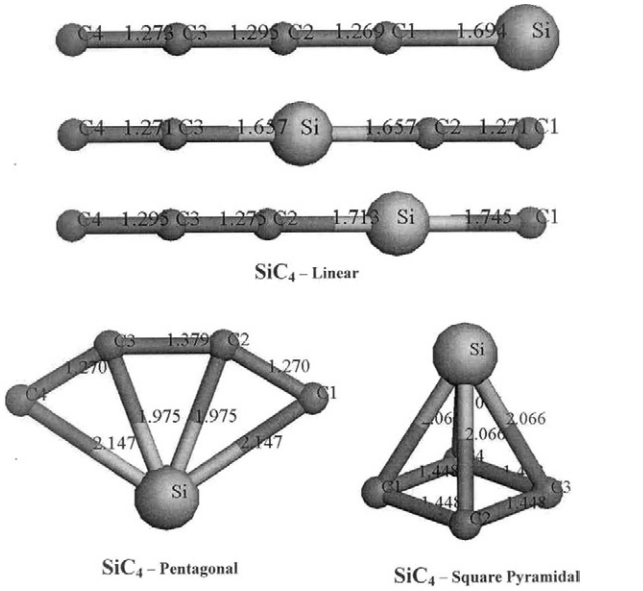

Figure 4. Optimized structures of SiC_4 nanoclusters.

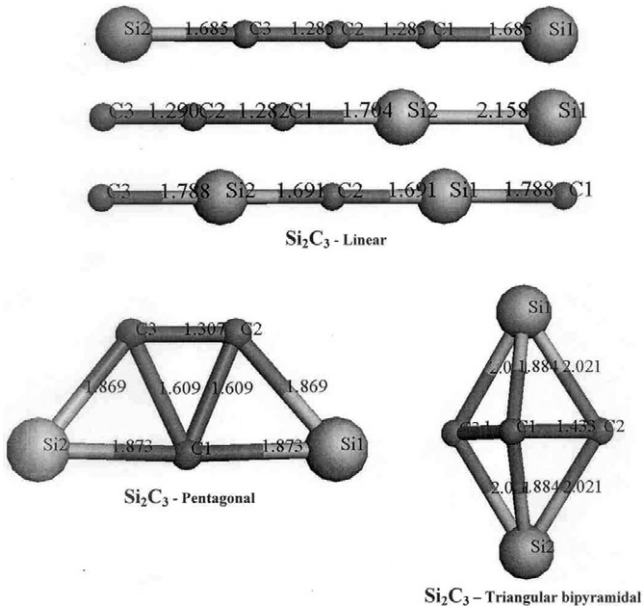

Figure 5. Optimized structures of Si_2C_3 nanoclusters.

Si–Si bond lengths and the bond angle SiCSi, 144° are similar to those calculated by Rittby [45] and Li *et al* [37].

Si_mC_n $(m + n = 4)$

All the structures have the triplet ground states except the SiC_3 rhomboidal, Si_2C_2 rhombus and tetrahedral and Si_3C rhomboidal and triangular pyramidal structures, which have singlet ground states.

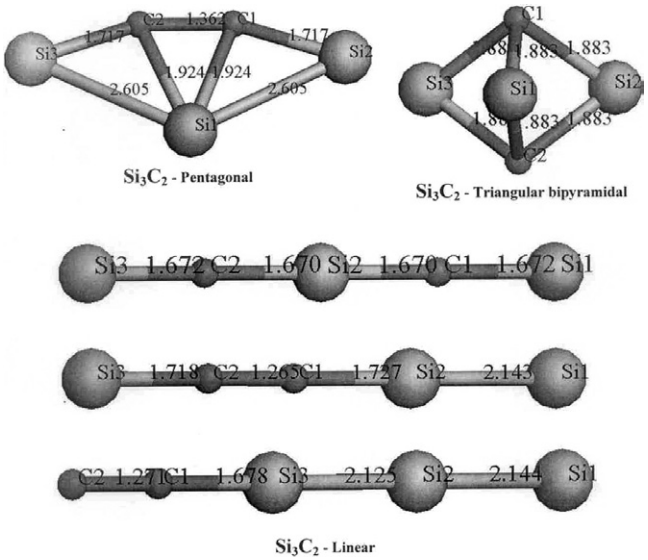

Si_3C_2 - Pentagonal

Si_3C_2 - Triangular bipyramidal

Si_3C_2 - Linear

Figure 6. Optimized structures of Si_3C_2 nanoclusters.

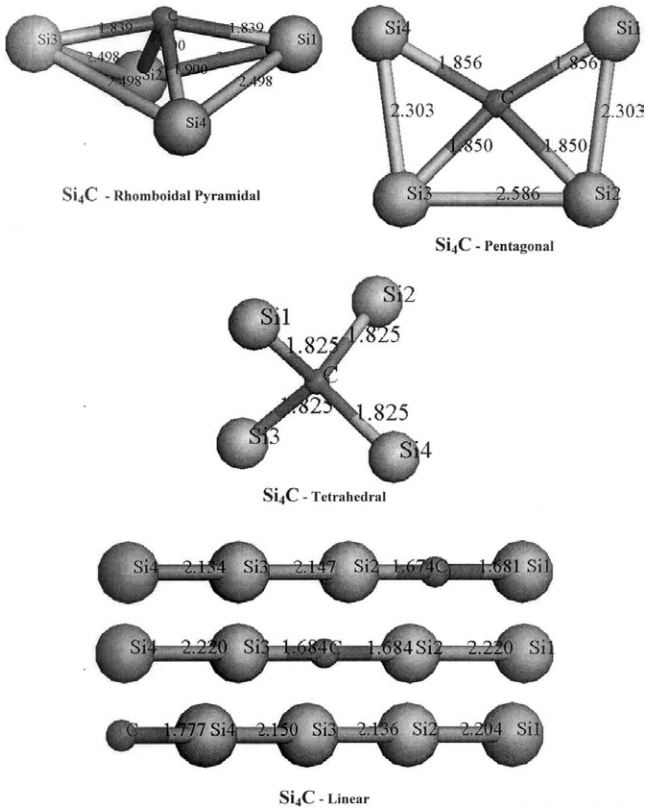

Si_4C - Rhomboidal Pyramidal

Si_4C - Pentagonal

Si_4C - Tetrahedral

Si_4C - Linear

Figure 7. Optimized structures of Si_4C nanoclusters.

Table 1. Binding energy (BE) per atom, HOMO–LUMO gap (eV), ionization potential (IP) and adiabatic electron affinity (EA) in eV for all the configurations of Si_mC_n ($2 \leqslant m+n \leqslant 5$) clusters. The most stable configurations are bold-faced ones.

Cluster	Configuration	BE without zero point energy	Zero point energy	BE with zero point energy	HOMO–LUMO gap	IP	EA		
							Present	Expt	Others [48]
SiC	**Linear**	**2.18**	**0.06**	**2.12**[a]	**1.96**	**8.89**	**2.10**		
SiC_2	**Linear (SiCC)**	**4.25**	**0.17**	**4.08**	**3.90**	**9.69**	**1.50**	**1.37** [27]	**1.15**
	Triangular	**4.25**	**0.17**	**4.08**	**3.84**	**9.79**	**1.17**		**0.97**
	Linear (CSiC)	2.15			2.51				
Si_2C	**Linear (SiCSi)**	**3.62**	**0.12**	**3.50**	**4.11**	**9.18**	**1.10**		
	Triangular	**3.62**	**0.13**	**3.49**	**4.19**	**9.19**	**1.01**		
	Linear (CSiSi)	2.18			2.40				
SiC_3	**Linear (SiCCC)**	**4.55**	**0.31**	**4.24**	**2.39**	**9.04**	**2.51**	**2.64** [27]	**2.55**
	Rhomboidal	4.42	0.29	4.13	2.75	8.99	1.98		
	Triangular pyramidal	4.18			2.73				
	Linear (CSiCC)	3.70			2.82				
Si_2C_2	**Rhombus**	**4.18**	**0.26**	**3.92**	**3.65**	**8.97**	**1.29**		
	Linear (SiCCSi)	**4.18**			**1.98**				
	Tetrahedral	3.64			1.93				
	Linear (SiSiCC)	3.62			2.26				
	Linear (SiCSiC)	3.26			2.82				
Si_3C	**Rhomboidal**	**3.65**	**0.19**	**3.46**	**2.90**	**7.81**	**1.44**		
	Triangular pyramidal	3.42			2.02				
	Linear (SiCSiSi)	3.15			2.11				
	Linear (SiSiSiC)	2.29			2.22				
SiC_4	**Linear (SiCCCC)**	**5.10**	**0.47**	**4.63**	**3.52**	**9.49**	**2.17**	**2.15** [27]	**1.40**
	Pentagonal	4.88			4.25				
	Linear (CCSiCC)	4.57			4.21				
	Square pyramidal	4.05			2.62				
	Linear (CCCSiC)	4.02			2.16				
Si_2C_3	**Linear (SiCCCSi)**	**4.77**	**0.42**	**4.35**	**3.11**	**8.12**	**1.63**	**1.50** [27], **1.77** [51]	
	Pentagonal	4.29			2.16				
	Linear (CCCSiSi)	4.04			2.09				
	Triangular bipyramidal	3.88			1.83				
	Linear (CSiCSiC)	2.83			2.094				
Si_3C_2	**Pentagonal**	**4.13**	**0.32**	**3.81**	**2.71**	**7.27**	**1.41**		
	Triangular bipyramidal	3.91			4.13				
	Linear (SiCSiCSi)	3.87			3.77				
	Linear (SiCCSiSi)	3.77			1.84				
	Linear (CCSiSiSi)	3.38			2.46				
Si_4C	Rhomboidal pyramidal	3.49	0.22	3.27	2.15	8.49	2.28		
	Pentagonal	**3.39**	**0.22**	**3.17**	**1.65**	**6.70**	**1.80**		
	Linear (SiCSiSiSi)	3.02			2.37				
	Tetrahedral	3.01			2.04				
	Linear (SiSiCSiSi)	2.80			1.27				
	Linear (SiSiSiSiC)	2.18			0.92				

[a] Expt value = 2.30 eV [42].

Table 2. Bond lengths (in Å) of small Si_mC_n ($2 \leqslant m + n \leqslant 4$) clusters. ([37]—B3LYP-DFT/6-311G(3df), [43]—SCF, [44]—MBPT(2), [45]—MBPT2/6-311G(2d), HF/6-31G*, MBPT(2)/DZP, [46]—MCSCF, [47]—DZP, [49]—MBPT2/6-311G*, [50]—CCSD(T)/cc-pVQZ, [51]—HF/cc-pVDZ, B3LYP/cc-pVDZ, [52]—B3LYP/6-311G(2d), 6-31G*.)

Cluster	Structure	Bonds	Present	Others	Expt
SiC	Linear	Si–C	1.713	1.71 [37], 1.734 [13]	1.731 [13]
SiC_2	Linear	Si–C	1.692	1.705 [44], 1.676 [43]	
	(SiCC)	C–C	1.277	1.301 [44], 1.273 [43]	
	Triangular	Si–C	1.84	1.84 [37], 1.835 [43, 44]	1.837 [11], 1.812 [36]
		C–C	1.26	1.256 [43], 1.294 [44]	1.268 [11], 1.250 [36]
Si_2C	Linear (SiCSi)	Si–C	1.689	1.702 [45]	
	Triangular	Si–C	1.689	1.69 [37], 1.703 [45]	
		Si–Si	3.217		
SiC_3	Linear	Si–C_1	1.728	1.75 [46], 1.696 [47]	
	(SiCCC)	C_1–C_2	1.284	1.30 [46], 1.285 [47]	
		C_2–C_3	1.303	1.32 [46], 1.303 [47]	
	Rhomboidal	Si–C_1(C_2)	2.041	2.06 [46], 2.021 [47]	2.022 [17]
		Si–C_3	1.895	1.89 [46], 1.882 [47]	1.893 [17]
		C_3–C_1(C_2)	1.334	1.32 [46], 1.325 [47]	1.344 [17]
Si_2C_2	Rhombus	Si–C	1.832	1.836 [49], 1.82 [46]	
		C–C	1.429	1.464 [49], 1.48 [46]	
		Si–Si	3.373	3.33 [46]	
	Linear	Si–C	1.737	1.735 [49], 1.77 [46]	
	(SiCCSi)	C–C	1.272	1.287 [49], 1.27 [46]	
Si_3C	Rhomboidal	Si_2(Si_3)–C	1.757	1.795 [45], 1.739 [45]	
		Si_1–C	1.935	1.973 [45], 1.930 [45]	
		Si_1–Si_2(Si_3)	2.438	2.448 [45], 2.438 [45]	
SiC_4	Linear	Si–C_1	1.694	1.693 [50]	1.682 [50]
	SiCCCC	C_1–C_2	1.269	1.273 [50]	1.280 [50]
		C_2–C_3	1.295	1.299 [50]	1.299 [50]
		C_3–C_4	1.273	1.281 [50]	1.274 [50]
Si_2C_3	Linear	Si–C	1.685	1.66 [45], 1.704 [51], 1.672 [51]	
	(SiCCCSi)	C–C	1.285	1.283 [45], 1.297 [51], 1.287 [51]	
Si_3C_2	Pentagonal	C_1–C_2	1.362	1.362 [52]	
		Si_2–C_1	1.717	1.719 [52]	
		Si_3–C_2	1.717	1.719 [52]	
		Si_1–C_1(C_2)	1.924	1.934 [52]	
		Si_1–Si_2(Si_3)	2.605	2.620 [52]	
Si_4C	Rhomboidal	Si–Si	2.498		
	pyramidal	Si_1(Si_3)–C	1.839		
		Si_2(Si_4)–C	1.900		
	Pentagonal	Si_1–Si_2	2.302		
		Si_3–Si_4	2.302		
		Si_2–Si_3	2.586		
		Si_1(Si_4)–C	1.856		
		Si_2(Si_3)–C	1.85		

SiC_3. We have investigated four different configurations: two linear chains Si–C–C–C ($C_{\infty v}$) and C–Si–C–C ($C_{\infty v}$), rhomboidal (C_{2v}) and triangular pyramidal (C_s) ones. The linear

Si–C–C–C and the rhomboidal geometries have quite similar BEs. Rintelman *et al* [46] and some others [47, 48] have also made similar observations. For the linear SiCCC our calculated EA (2.51 eV) is in very good agreement with the experimental value equal to 2.64 eV [27]. Also the present Si–C_1, C_1–C_2 and C_2–C_3 bond lengths are close to the others [46, 47]. Similarly, the calculated bond lengths for the rhomboidal structure are in good agreement with those of the experimental [17] and other theoretical values [46, 47]. Our calculated $C_1C_3C_2$ and C_1SiC_2 bond angles are 152.37° and 78.81°, respectively. One of them is similar to a value of 152.3° reported by Alberts *et al* [47].

Si_2C_2. We have studied three linear chains, Si–C–C–Si ($D_{\infty h}$), Si–Si–C–C ($C_{\infty v}$) and Si–C–Si–C ($C_{\infty v}$), planar rhombus (D_{2h}) and tetrahedral (C_{2v}) configurations. The rhombus and the linear Si–C–C–Si have quite similar BEs. The currently calculated values of the Si–Si, Si–C and C–C bond lengths for the rhombus and the linear SiCCSi configurations are close to those of others [46, 49], as can be seen in the tables.

Si_3C. We have considered the rhomboidal (C_{2v}), triangular pyramidal (C_s) and two linear SiSiSiC ($C_{\infty v}$) and SiCSiSi ($C_{\infty v}$) configurations and find the rhomboidal one as the most stable configuration. The present $Si_2(Si_3)$–C, Si_1–C and Si_1–$Si_2(Si_3)$ bond lengths are quite close to the values reported by Rittby [45]. The SiCSi and SiSiSi bond angles are 165° and 91°, respectively, which are quite close to the values of 161.8°, 166.2°, and 92.8°, 90.1°, respectively, as reported by Rittby [45].

Si_mC_n $(m + n = 5)$

Here all the structures have singlet ground states except the Si_2C_3 pentagonal and linear CSiCSiC and Si_4C linear SiSiCSiSi and SiSiSiSiC structures, which have triplet ground states.

SiC_4. Five different geometries, pentagonal (C_{2v}), square pyramidal (C_{4v}), and three linear chains SiCCCC ($C_{\infty v}$), CCSiCC ($D_{\infty h}$) and CCCSiC ($C_{\infty v}$), were considered. The linear chain SiCCCC is the most stable structure. For this structure, our calculated EA of 2.17 eV is in excellent agreement with the available experimental result 2.14 eV [27]. The different predicted bond lengths are in excellent agreement with the experimental values [50].

Si_2C_3. We have studied five configurations, namely the pentagonal (C_{2v}), triangular bipyramidal (C_{2v}) and three linear chains SiCCCSi ($D_{\infty h}$), CCCSiSi ($C_{\infty v}$) and CSiCSiC ($D_{\infty h}$). Among them the linear chain SiCCCSi is the most stable one. The predicted value of EA (1.63 eV) is in good agreement with the experimental values, 1.766 and 1.50 eV [27, 51]. Our calculated Si–C and C–C bond lengths are quite close to the values reported by others [45, 51].

Si_3C_2. Again five different structures are investigated, which are pentagonal (C_{2v}), triangular bipyramidal (C_{2v}) and three linear chains SiCSiCSi ($D_{\infty h}$), SiCCSiSi ($C_{\infty v}$) and CCSiSiSi ($C_{\infty v}$). Out of these the planar pentagonal structure is the most stable one. The present C_1–C_2, Si_2–C_1, Si_3–C_2, Si_1–$C_1(C_2)$ and Si_1–$Si_2(Si_3)$ bond lengths are in good agreement with others [52].

Si_4C. Six different geometries, the rhomboidal pyramidal (C_{2v}), pentagonal (C_{2v}), centred tetrahedral (T_d) and three linear chains SiCSiSiSi ($C_{\infty v}$), SiSiCSiSi ($D_{\infty h}$) and SiSiSiSiC ($C_{\infty v}$), have been investigated. All the structures have lower BEs than the other five atom nanoclusters. The rhomboidal pyramidal and pentagonal structures are seen to have quite similar BEs.

Our currently calculated data for the bond lengths and bond angles are in close agreement with those of others.

The variation of the BEs/atom with the cluster size $(m+n)$ has been depicted in figure 8(a). In figure 8 the superscripts l, r, t and p denote the linear chain, rhomboidal, triangular and pentagonal structures, respectively. A perusal of figure 8(a) reveals that the most stable structures are those which contain the maximum number of carbon atoms having the strongest

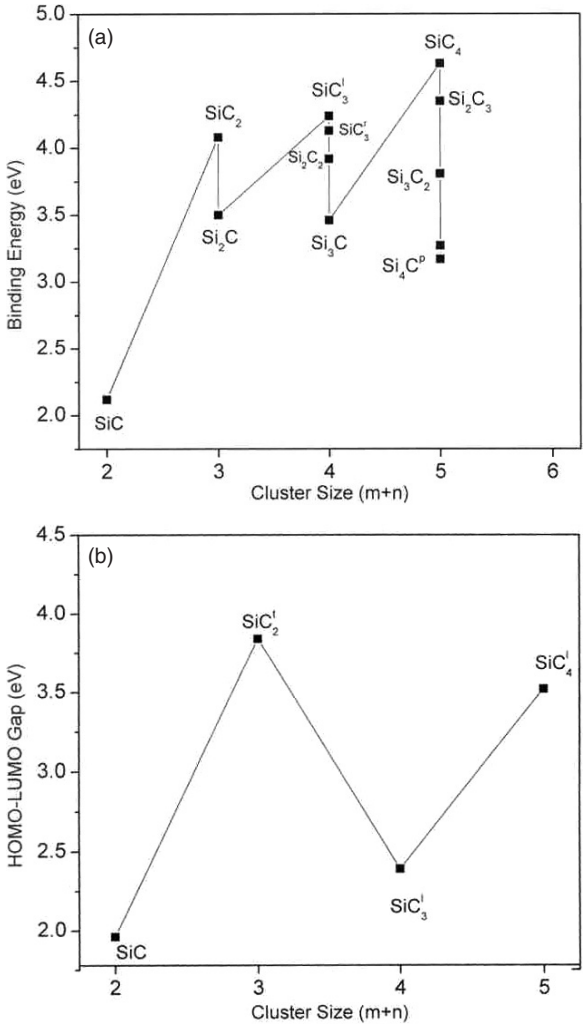

Figure 8. Variation of (a) BEs and (b) HOMO–LUMO gap with the cluster size ($m + n$).

C–C bonds, whereas the lowest binding is seen for clusters containing large numbers of silicon atoms and the resulting weak Si–Si bonds. For the clusters containing large numbers of carbon atoms and one silicon atom the BE increases monotonically with the number of carbon atoms.

3.2. Electronic properties

HOMO–LUMO gap. The variation of HOMO–LUMO gap with the cluster size for the most stable structures has been shown in figure 8(b). One observes that the clusters containing even numbers of carbon atoms are much stronger than those clusters containing odd numbers of carbon atoms.

Ionization potential and electron affinity. The ionization potential (IP) is defined as the amount of energy required to remove an electron from a cluster. This is computed as the energy difference between the cationic and the neutral clusters. The variation of IP with the cluster size

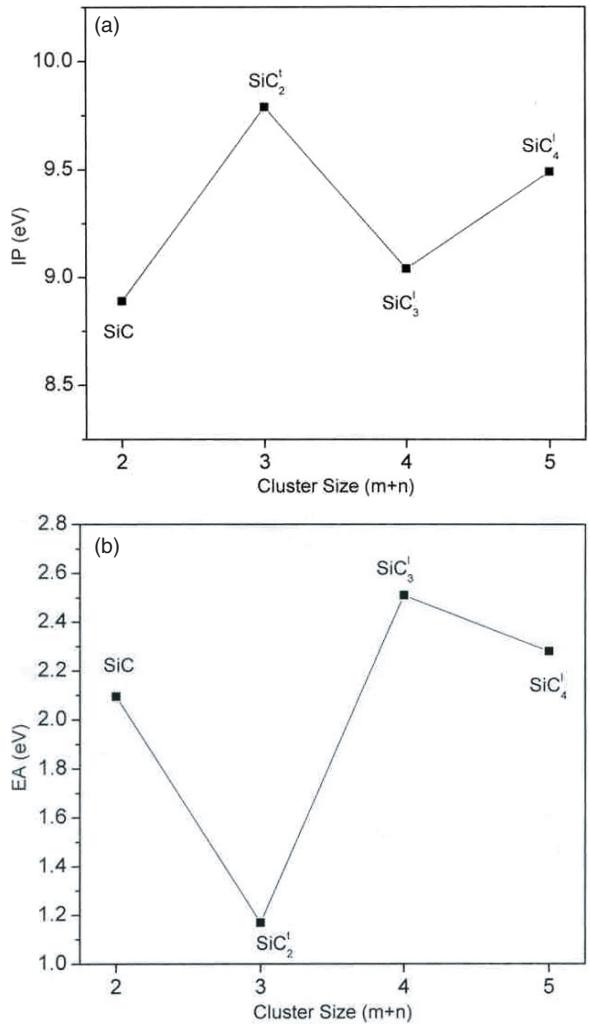

Figure 9. Variation of (a) IP and (b) EA with the cluster size ($m + n$).

has been presented in figure 9(a). The superscripts are similar to figure 8. We observe that the IP again shows a zigzag behaviour. The IPs for the clusters containing even numbers of carbon atoms are greater than the clusters containing odd numbers of carbon atoms.

The adiabatic electron affinity (EA) is defined as the energy released when an electron is added to a neutral cluster. We have computed it as the energy difference between the neutral and the anionic clusters. The variation of EA with the cluster size is shown in figure 9(b). A behaviour different from the variation of HOMO–LUMO gap and IP is observed. The EA is now greater for the clusters containing odd numbers of carbon atoms as compared to those clusters which contain even numbers of carbon atoms.

The ground states of the clusters containing even numbers of carbon atoms are in general lower than those containing odd numbers of carbon atoms, whereas the lowest unoccupied states of the clusters containing even numbers of carbon atoms lie higher than those containing odd numbers of carbon atoms.

Table 3. Si_mC_n ($2 \leqslant m + n \leqslant 3$) clusters, the calculated vibrational frequencies (cm^{-1}), infrared intensities (IR int. in km mol^{-1}), relative IR intensities (Rel. IR int.) and Raman scattering activities (Raman activity in A^4/amu). Brackets following the frequencies contains the multiplicity of the mode. ([37]—B3LYP-DFT/6-311G(3df), [43]—SCF, Reference [44]—MBPT(2), [45]—MBPT2/6-311G(2d), [48]—MBPT2/6-311G*.)

Configuration		Properties	Values
Linear (SiC)		Frequency	987
	Present	IR int.	14.87
		Rel. IR int.	1.0
		Raman activity	233.84
	Others	Frequency [13]	927
		Frequency [37]	986
Linear (SiCC)		Frequencies	25i (2), 800, 1929
	Present	IR int.	1.85, 41.64, 681.31
		Rel. IR int.	0.00, 0.06, 1.0
		Raman activity	0.21, 84.48, 20.60
	Others	Frequencies [44]	147, 787, 1904
		Frequencies [43]	173, 876, 2054
Triangular		Frequencies	148, 802, 1839
(SiC_2)	Present	IR int.	87.63, 147.94, 24.12
		Rel. IR int.	0.59, 1.0, 0.16
		Raman activity	9.87, 32.81, 29.39
	(Expt)	Frequencies [53]	160.4, 824.3, 1741.3
		Frequencies [43]	328i, 851, 1976
	Others	Frequencies [44]	183, 840, 1720
		Frequencies [48]	161, 840, 1759
Linear		Frequencies	15i (2), 585, 1406
(SiCSi)	Present	IR int.	3.44, 0.0, 545.13
		Rel. IR int.	0.0, 0.0, 1.0
		Raman activity	0.0, 138.62, 0.0
	Others	Frequencies [45]	99i, 559, 1368
Triangular		Frequencies	47, 695, 1357
(Si_2C)	Present	IR int.	3.63, 8.52, 430.49
		Rel. IR int.	0.01, 0.02, 1.0
		Raman activity	9.67, 129.14, 6.78
	Expt	Frequencies [53]	839.5, 1188.4
		Rel. IR int. [53]	0.07, 1.0
	Others	Frequencies [45]	131, 808, 1223
		Rel. IR int. [45]	0.01, 0.07, 1.0

3.3. Vibrational frequencies

The vibrational frequencies are calculated using the B3LYP-DFT/6-311G(3df) method for the most stable nanoclusters. We calculate the second derivative of total energy of the system with respect to atomic displacements. The obtained dynamical matrix is diagonalized. We have also calculated the infrared intensities (IR int.), relative infrared intensities (Rel. IR int.) and Raman scattering activities (Raman activity). The above calculated physical quantities for the two and three atom clusters are presented in table 3, for four atom clusters in table 4 and for five atom clusters in table 5, respectively. In these tables, the brackets following the frequencies contain the multiplicity of the mode. We discuss each nanocluster below:

Table 4. Si_mC_n $(m+n=4)$ clusters, calculated vibrational frequencies (cm^{-1}), infrared intensities (IR int. in km mol^{-1}), relative intensities (Rel. IR int.) and Raman scattering activities (Raman activity in A^4/amu). Brackets following the frequencies contain the multiplicity of the mode. ([45]—MBPT(2)/DZP, [46]—MCSCF, [47]—DZP, TZ2P, [48]—MP2/6-31G*, [49]—MBPT2/6-311G*.)

Configuration		Properties	Values
Linear		Frequencies	150 (2), 396 (2), 625, 1333, 1986
(SiCCC)	Present	IR int.	1.88, 9.61, 13.91, 62.63, 160.5
		Rel. IR int.	0.01, 0.06, 0.09, 0.39, 1.0
		Raman activity	0.11, 2.06, 160.55, 0.13, 445.74
	Others	Frequencies [48]	151, 380, 629, 1332, 2003
		Frequencies [47]	171, 474, 681, 1285, 2033
Rhomboidal		Frequencies	194, 391, 503, 797, 1160, 1597
(SiC_3)	Present	IR int.	50.63, 3.61, 19.63, 47.88, 0.43, 57.10
		Rel. IR int.	0.89, 0.06, 0.34, 0.84, 0.01, 1.0
		Raman activity	0.0, 9.30, 14.10, 16.29, 53.15, 0.43
	Others	Frequencies [46]	279, 420, 538, 852, 1254, 1603
		Frequencies [47]	341, 439, 588, 859, 1277, 1623; 308, 419, 575, 849, 1262, 1622
Rhombus		Frequencies	201, 367, 512, 974, 985, 1133
(Si_2C_2)	Present	IR int.	2.96, 53.37, 0.0, 0.0, 307.40, 0.0
		Rel. IR int.	0.01, 0.17, 0.0, 0.0, 1.0, 0.0
		Raman activity	0.0, 0.0, 110.99, 6.09, 0.0, 24.72
	Expt	Frequencies [49]	382.2, 982.9
		Rel. IR int. [49]	0.18, 1.0
	Others	Frequencies [49]	213, 397, 522, 978, 1011, 1067
		IR int. [49]	4.0, 61.0, 0.0, 0.0, 287, 0.0
		Rel. IR int. [49]	0.01, 0.21, 0.0, 0.0, 1.0, 0.0
		Frequencies [46]	224, 424, 543, 1013, 1026, 1066
Linear		Frequencies	123 (2), 370 (2), 481, 907, 1843
(SiCCSi)	Present	IR int.	2.496, 0.0, 0.0, 5.844, 0.0
		Rel. IR int.	0.43, 0.0, 0.0, 1.0, 0.0
		Raman activity	0.0, 0.323, 333.31, 0.0, 2016.07
	Expt	Frequencies [49]	957
	Others	Frequencies [49]	117, 278, 493, 933, 1801
		IR int. [49]	4.0, 0.0, 0.0, 197.0, 0.0
		Rel. IR int. [49]	0.02, 0.0, 0.0, 1.0, 0.0
Rhomboidal		Frequencies	179, 299, 340, 513, 656, 1114
(Si_3C)	Present	IR int.	0.01, 5.61, 11.26, 22.31, 51.29, 66.31
		Rel. IR int.	0.0, 0.08, 0.17, 0.34, 0.77, 1.0
		Raman activity	0.06, 20.90, 7.07, 77.11, 45.35, 10.63
	Expt	Frequencies [53]	310, 358, 512, 658, 1101
		Rel. IR int. [53]	0.11, 0.16, 0.32, 0.52, 1.0
	Others	Frequencies [45]	184, 307, 377, 494, 646, 1107
		Rel. IR int. [45]	0.0, 0.05, 0.11, 0.19, 0.48, 1.0

SiC. We predict the stretching mode frequency at 987 cm^{-1}, which is quite close to 986 cm^{-1} [37] and far from 927 cm^{-1} reported by others [13]. This stretching frequency is both IR and Raman active.

Si_mC_n $(m+n=3)$

For the two three atom linear chain structures, SiC_2 and Si_2C, we find that the lowest transverse frequencies are imaginary, making them unstable.

Table 5. Si_mC_n ($m + n = 5$) clusters, the calculated vibrational frequencies (cm^{-1}), infrared intensities (IR int. in km mol^{-1}), relative intensities (Rel. int.) and Raman scattering activities (Raman activity in A^4/amu). Brackets following the frequencies contain the multiplicity of the mode. ([45]—MBPT(2)/DZP, [50]—CCSD(T)/cc-pVQZ, [51]—B3LYP/cc-pVDZ, [52]—B3LYP/6-311G(2d).)

Configuration		Properties	Values
Linear		Frequencies	93(2), 219(2), 568(2), 581, 1188, 1893, 2179
(SiCCCC)	Present	IR int.	0.27, 8.80, 6.13, 31.78, 112.14, 16.66, 2681.91
		Rel. IR int.	0.0, 0.0, 0.0, 0.01, 0.04, 0.01, 1.0
		Raman activity	0.93, 0.85, 0.02, 164.07, 2.01, 378.43, 37.06
	(Expt)	Frequencies [15]	2080.1
	Others	Frequencies [50]	88, 206, 547, 571, 1168, 1852, 2144
Linear		Frequencies	82 (2), 204 (2), 472, 573 (2), 923, 1589, 2044
(Si_2C_3)	Present	IR int.	4.32, 0.0, 0.0, 12.36, 204.34, 0.0, 2499.28
		Rel. IR int.	0.0, 0.0, 0.0 0.01, 0.08, 0.0, 1.0
		Raman activity	0.0, 2.25, 271.49, 0.0, 0.0, 757.51, 0.0
		Frequencies [53]	899, 1955
	(Expt)	Rel. IR int. [53]	0.07, 1.0
		Frequencies [51]	490 ± 25, 1520 ± 25
	Others	Frequencies [45]	85, 210, 442, 519, 869, 1527, 2082
		Rel. IR int. [45]	0.0, 0.0, 0.0, 0.01, 0.06, 0.0, 1.0
		Frequencies [51]	84, 206, 466, 580, 904, 1577, 2052
		Rel. IR int. [51]	0.0, 0.0, 0.0, 0.01, 0.09, 0.0, 1.0
Pentagonal		Frequencies	153, 158, 167, 456, 469, 603, 686, 988, 1505
(Si_3C_2)	Present	IR int.	2.20, 1.32, 1.10, 0.0, 5.24, 39.44, 33.43, 52.28, 0.56
		Rel. IR int.	0.04, 0.03, 0.02, 0.0, 0.10, 0.75, 0.64, 1.0, 0.01
		Raman activity	0.15, 7.42, 15.51, 1.62, 73.74, 8.36, 142.26, 1.84, 905.86
	(Expt)	Frequencies [52]	599, 681, 957
		Rel. IR int. [52]	0.98, 0.31, 1.0
	Others	Frequencies [52]	152, 156, 167, 449, 466, 586, 674, 982, 1497
		Rel. IR int. [52]	0.04, 0.01, 0.02, 0.0, 0.12, 0.78, 0.69, 1.0, 0.01
Rhomboidal		Frequencies	92i, 189, 204, 259, 287, 443, 638, 754, 787
pyramidal	Present	IR int.	10.95, 0.24, 0.0, 0.40, 0.05, 11.57, 16.95, 161.83, 0.33
(Si_4C)		Rel. IR int.	0.07, 0.0, 0.0, 0.0, 0.0, 0.07, 0.10, 1.0, 0.0
		Raman activity	5.35, 7.86, 14.20, 6.31, 29.27, 75.10, 48.97, 2.57, 0.73
Pentagonal		Frequencies	47, 103, 131, 299, 336, 343, 498, 853, 861
(Si_4C)	Present	IR int.	14.66, 2.86, 0.0, 10.66, 0.78, 8.12, 2.76, 16.76, 105.76
		Rel. IR int.	0.14, 0.03, 0.0, 0.10, 0.01, 0.07, 0.02, 0.16, 1.0
		Raman activity	0.39, 2.33, 0.06, 9.44, 10.59, 68.89, 142.78, 0.34, 4.56

SiC_2. For the triangular structure, our calculated symmetric, antisymmetric and bending vibrational frequencies are near to the experimental data and the maximum discrepancy lies within 8%. All the vibrational modes are both IR and Raman active.

Si_2C. For the triangular structure, our predicted vibrational frequencies of 47, 695 and 1357 cm^{-1} are close to the experimental values of 839.5 and 1188.4 cm^{-1} [53] as presented in table 3. The lowest frequency has not been reported in the experiments. The present Rel. IR int. are very near to the experimental data [53]. Here, the nature of vibrations of the highest and lowest frequencies is interchanged because of the large mass of silicon as compared to the carbon atom.

Si_mC_n ($m + n = 4$)

SiC_3. For the linear SiCCC structure, our calculated seven vibrational frequencies are real and are in good agreement with the values reported by Alberts *et al* [47] and Gomei *et al* [48].

For the rhomboidal structure, all the six frequencies are somewhat lower than those of others [46, 47].

Si_2C_2. Two out of six calculated vibrational frequencies, namely 367 and 985 cm^{-1}, obtained for the rhombus structure are in good agreement with the measured frequencies of 382.2 and 982.9 cm^{-1} [49]. Also the calculated Rel. IR int. for these two frequencies are in very good agreement with the available experimental values [49].

For the linear SiCCSi chain, the present frequency of 907 cm^{-1} is near to the experimental frequency of 957 cm^{-1} proposed by Presilla-Marquez *et al* [49]. However, large discrepancies are seen between our calculated IR int. and Raman activity and those of Presilla-Marquez *et al* [49].

Si_3C. Our five frequencies 299, 340, 513, 656 and 1114 cm^{-1} for the rhomboidal configuration are in excellent agreement with the experimental values of 310, 358, 512, 658 and 1101 cm^{-1} [53]. Also, our calculated Rel. IR int. for these frequencies are in very good agreement with the experiment [53].

Si_mC_n $(m + n = 5)$

SiC_4. For the linear Si–C–C–C-C structure, our calculated highest vibrational frequency, 2179 cm^{-1}, is in close agreement with the experimental value of 2080.1 cm^{-1} [15], and other calculated frequencies are in good agreement with the values reported by Gordon *et al* [50].

Si_2C_3. For the linear Si–C–C–C-Si, four out of ten frequencies, namely 472, 923, 1589 and 2044 cm^{-1}, are in close agreement with the measured data of 490 ± 25, 899, 1520 ± 25 and 1955 cm^{-1} [51, 53]. Also, our calculated Rel. IR int. for the two frequencies of 923 and 2044 cm^{-1} are close to the experimental data [53].

Si_3C_2. For the pentagonal structure, our calculated vibrational frequencies of 603, 686 and 988 cm^{-1} are in excellent agreement with the experimental values of 599, 681 and 957 cm^{-1} [52]. Our calculated Rel. IR int. of 0.75, 0.64 and 1.0 for these frequencies are in reasonable agreement with the experimental values of 0.98, 0.31 and 1.0 [52].

Si_4C. For the rhomboidal pyramidal structure, the lowest frequency out of nine calculated frequencies is imaginary. The structure may thus be unstable. For the pentagonal structure, all the frequencies are real.

In the above discussion, we find that although two of the linear chains, namely SiCC and SiCSi and the rhomboidal pyramidal Si_4C structure, have high BEs, their lower frequencies are seen to be imaginary, which will result in their instability.

4. Conclusion

The present study establishes the occurrence of the most stable configurations of the various silicon–carbon nanoclusters. Some of the currently studied structures have not been discussed in the literature. For many Si_mC_n nanoclusters, we have predicted the bond lengths, binding energies, HOMO–LUMO gaps, IP, EA, vibrational frequencies, IR int., Rel. IR int. and Raman scattering activities, some of which need to be verified experimentally. The results are, in general, in good agreement with the experimental data wherever available.

The diatomic SiC molecule has very small BE. The most stable structures are those which contain the maximum number of carbon atoms because of the occurrence of the strongest C–C bonds, whereas the lowest binding is seen for clusters containing the maximum number of silicon atoms because of the occurrence of the maximum number of weak Si–Si bonds. For the clusters containing the maximum number of carbon atoms, i.e. the clusters containing only one silicon atom, the BE increases monotonically with the number of carbon atoms.

A general behaviour of the silicon–carbon clusters is seen that the ground states of the cluster containing even numbers of carbon atoms are in general lower than those containing

odd numbers of carbon atoms, whereas the lowest unoccupied states of the clusters containing even numbers of carbon atoms lie higher than those containing odd numbers of carbon atoms.

We find that although two linear chains, namely SiCC and SiCSi, and the rhomboidal pyramidal Si_4C structures have high BEs, as their low frequencies are imaginary they may not be stable.

Acknowledgments

The authors are thankful to University Grants Commissions and Defence Research and Development Organization, New Delhi, for financial assistance.

References

[1] Jarrold M F and Constant V A 1991 *Phys. Rev. Lett.* **67** 2994
[2] Liu B, Lu Z Y, Pan B, Wang C Z and Ho K M 1998 *J. Chem. Phys.* **109** 9401
[3] Ho K M, Shvartsberg A A, Pan B, Lu Z Y, Wang C Z, Wacker J G, Fye J L and Jarrod M F 1998 *Nature* **392** 582
[4] Hunter J M, Fye J L and Jarrod M F 1994 *Phys. Rev. Lett.* **73** 2063
[5] Shvartsberg A A and Jarrod M F 1999 *Phys. Rev.* A **60** 1235
[6] Lu Z-Y, Wang C-Z and Ho K-M 2000 *Phys. Rev.* B **61** 2329
[7] Melinon P, Keghelian P, Perez A, Ray C, Lerme J, Pellarin M, Broyer M, Boudeulle M, Champagnon B and Rousset J L 1998 *Phys. Rev.* B **58** 16481
[8] Melinon P, Paillard V, Dupuis V, Perez A, Jensen P, Hoareau A, Broyer M, Vialle J L, Pellarin M, Baguenard B and Lerme J 1995 *Int. J. Mod. Phys.* B **9** 339
[9] Bernhard N and Bauer G H 1995 *Phys. Rev.* B **52** 8829
[10] Cernicharo J, Gottlieb C A, Guelin M, Thaddeus P and Vrtilek J M 1989 *Astrophys. J.* **341** L25
[11] Thaddeus P, Cummins S E and Linke R A 1984 *Astrophys. J.* **283** L45
[12] Ohishi M, Kaifu N, Kawaguchi K, Murakami A, Saito S, Yumamoto S, Ishikawa S-I, Fujitu Y, Shiratori Y and Ievine W M 1989 *Astrophys. J.* **345** L83
[13] Bernath P F, Rogers S A, O'Brien L C, Brazier C R and McLean A D 1998 *Phys. Rev. Lett.* **60** 197
[14] Apponi A J, McCarthy M C, Gottlieb C A and Thaddeus P 1999 *Astrophys. J.* **516** L103
[15] Withey P A and Graham W R M 1992 *J. Chem. Phys.* **96** 4068
[16] Van Orden A, Giesen T F, Provencal R A, Hwang H J and Saykally R J 1994 *J. Chem. Phys.* **101** 10237
[17] McCarthy M C, Apponi A J and Thaddeus P 1999 *J. Chem. Phys.* **110** 10645
McCarthy M C, Apponi A J and Thaddeus P 1999 *J. Chem. Phys.* **111** 7175
[18] McCarthy M C, Apponi A J, Gottlieb C A and Thaddeus P 2000 *Astrophys. J.* **538** 766
[19] Raghavachari K and Binkley J S 1987 *J. Chem. Phys.* **87** 2191 and references therein
[20] Shen L N and Graham W R M 1989 *J. Chem. Phys.* **91** 5115
[21] Arnold D W, Bradforth S E, Kitsopoulos T N and Neumark D M 1991 *J. Chem. Phys.* **95** 8753
[22] Li S, Van Zee R J, Weltner W Jr and Raghavachari K 1995 *Chem. Phys. Lett.* **243** 275 and references therein
[23] Raghavachari K and Rohlfing C M 1991 *J. Chem. Phys.* **94** 3670
[24] Adamowicz L 1991 *Chem. Phys. Lett.* **185** 244
[25] Rohlfing C M and Raghavachari K 1992 *J. Chem. Phys.* **96** 2114
[26] Fye J L and Jarrold M F 1997 *J. Phys. Chem.* A **101** 1836
[27] Nakajima A, Taguwa T, Nakao K, Gomei M, Kishi R, Iwata S and Kaya K 1995 *J. Chem. Phys.* **103** 2050
[28] Pellarin M, Ray C, Melinon P, Lerme J, Vialle J L, Keghelian P, Perez A and Broyer M 1997 *Chem. Phys. Lett.* **277** 96
[29] Pellarin M, Ray C, Lerme J, Vialle J L, Broyer M, Blasé X, Keghelian P, Melinon P and Perez A 1999 *J. Chem. Phys.* **110** 6927
[30] Suzuki H 1979 *Prog. Theor. Phys.* **62** 936
[31] Tsuji T 1965 *Ann. Tokyo Astron. Obs.* **9** 1
[32] McCabe E M 1982 *Mon. Not. R. Astron. Soc.* **200** 71
[33] Merill P W 1926 *Publ. Astron. Soc. Pac.* **38** 175
[34] Sanford R F 1926 *Publ. Astron. Soc. Pac.* **38** 177
[35] Kleman R 1956 *Astrophys. J.* **123** 162
[36] Michalopoulos D L, Geusic M E, Langridge P R R and Smalley R E 1984 *J. Phys. Chem.* **80** 3556

[37] Li S-D, Zhao Z-G, Zhao X-F, Wu H-S and Jin Z-H 2000 *Phys. Rev.* B **64** 195312
[38] Becke A D 1993 *J. Chem. Phys.* **98** 5648
Becke A D 1988 *Phys. Rev.* A **38** 3098
[39] Lee C, Yang W and Parr R G 1988 *Phys. Rev.* B **37** 785
[40] Miehlich B, Savin A, Stoll H and Preuss H 1989 *Chem. Phys. Lett.* **157** 200
[41] GAUSSIAN 03, Revision C.03, Gaussian, Inc., Pittsburgh PA, 2003
[42] Huber K P and Herzberg G 1979 *Constants of Diatomic Molecules* (New York: Van Nostrand-Reinhold)
[43] Grev R S and Schaefer H F III 1984 *J. Chem. Phys.* **80** 3552
[44] Fitzgerald G, Cole S J and Bartlett R J 1986 *J. Chem. Phys.* **85** 1701
[45] Rittby C M L 1991 *J. Chem. Phys.* **95** 5609
Rittby C M L 1992 *J. Chem. Phys.* **96** 6768
Rittby C M L 1994 *J. Chem. Phys.* **100** 175
[46] Rintelman J M and Gordan M S 2001 *J. Chem. Phys.* **115** 1795
[47] Alberts I L, Grev R S and Schaefer H F III 1990 *J. Chem. Phys.* **93** 5046
[48] Gomei M, Kishi R, Nakajima A, Iwata S and Kaya K 1997 *J. Chem. Phys.* **107** 10051
[49] Presilla-Marquez J D, Gay S C, Rittby C M L and Grahm W R M 1995 *J. Chem. Phys.* **102** 6354
[50] Gordon V D, Nathan E S, Apponi A J, McCarthy M C, Thaddeus P and Bostschwina P 2000 *J. Chem. Phys.* **113** 5311
[51] Duan X, Burggraf L W, Weeks D E, Davico G E, Schwartz R L and Lineberger W C 2002 *J. Chem. Phys.* **116** 3601
[52] Presilla-Marquez J D, Rittby C M L and Grahm W R M 1996 *J. Chem. Phys.* **104** 2818
[53] Presilla-Marquez J D and Grahm W R M 1990 *J. Chem. Phys.* **93** 5424
Presilla-Marquez J D and Grahm W R M 1991 *J. Chem. Phys.* **95** 5612
Presilla-Marquez J D and Grahm W R M 1992 *J. Chem. Phys.* **96** 6509
Presilla-Marquez J D and Grahm W R M 1994 *J. Chem. Phys.* **100** 181